



Nav1.8 in keratinocytes contributes to ROS-mediated inflammation in inflammatory skin diseases

Yiya Zhang^{a,b,c,1}, Yangfan Li^{a,b,1}, Lei Zhou^{a,b}, Xin Yuan^{a,b}, Yaling Wang^{a,b}, Qing Deng^{a,b}, Zhili Deng^{a,b}, San Xu^{a,b,c}, Qian Wang^d, Hongfu Xie^{a,b,c}, Ji Li^{a,b,c,*}

^a Department of Dermatology, Xiangya Hospital, Central South University, Changsha, China

^b Hunan Key Laboratory of Aging Biology, Xiangya Hospital, Central South University, Changsha, China

^c National Clinical Research Center for Geriatric Disorders, Xiangya Hospital, Central South University, Changsha, Hunan, 410008, China

^d Hunan Binsis Biotechnology Co., Ltd, Changsha, China

ARTICLE INFO

Keywords:

Nav1.8
ROS
SOD2
Rosacea
Psoriasis
Keratinocyte

ABSTRACT

Reactive oxygen species (ROS)-activated proinflammatory signals in keratinocytes play a crucial role in the immunoregulation of inflammatory skin diseases, including rosacea and psoriasis. Nav1.8 is a voltage-gated sodium ion channel, and its abnormal expression in the epidermal layer contributes to pain hypersensitivity in the skin. However, whether and how epidermal Nav1.8 is involved in skin immunoregulation remains unclear. This study was performed to identify the therapeutic role of Nav1.8 in inflammatory skin disorders. We found that Nav1.8 expression was significantly upregulated in the epidermis of rosacea and psoriasis skin lesions. Nav1.8 knockdown ameliorated skin inflammation in LL37- and imiquimod-induced inflammation mouse models. Transcriptome sequencing results indicated that Nav1.8 regulated the expression of pro-inflammatory mediators (IL1 β and IL6) in keratinocytes, thereby contributing to immune infiltration in inflammatory skin disorders. In vitro, tumor necrosis factor alpha (TNF α), a cytokine that drives the development of various inflammatory skin disorders, increased Nav1.8 expression in keratinocytes. Knockdown of Nav1.8 eliminated excess ROS production, thereby attenuating the TNF α -induced production of inflammatory mediators; however, a Nav1.8 blocker did not have the same effect. Mechanistically, Nav1.8 reduced superoxide dismutase 2 (SOD2) activity by directly binding to SOD2 to prevent its deacetylation and mitochondrial localization, subsequently inducing ROS accumulation. Collectively, our study describes a central role for Nav1.8 in regulating pro-inflammatory responses in the skin and indicates a novel therapeutic strategy for rosacea and psoriasis.

1. Introduction

Chronic inflammatory skin diseases, such as rosacea and psoriasis, are incurable and associated with considerable morbidity [1,2], causing a to physical, social, and emotional burden [2–4]. Although their pathogenesis remains poorly defined, inflammation and immune disturbance are central processes in these disorders, which is partly attributed to the production of proinflammatory mediators in keratinocytes [5,6].

Reactive oxygen species (ROS) are highly *reactive*, *oxygen*-containing molecules generated during cellular metabolism. ROS function as

signaling molecules involved in various biological processes and play a significant role in cellular homeostasis [7,8]. Excessive ROS levels have been reported to contribute to physiological and pathophysiological conditions by mediating inflammatory signaling pathways [9]. ROS are mainly generated by the *mitochondria* and *are regulated* by antioxidant enzymes [10]. Superoxide dismutase 2 (SOD2), an important antioxidant enzyme, is a natural defense against oxidative stress. It eliminates ROS and is, therefore, anti-inflammatory [11,12]. SOD2 is synthesized in the cytosol and imported into the mitochondria, where it is activated to scavenge ROS [13]. Moreover, deacetylation at lysine K68 is essential for SOD2 activity [14]. Recently, oxidative stress was reported to play an

Abbreviations: IMQ, imiquimod; ROS, reactive oxygen species; NC, negative control; DRG, dorsal root ganglion; TTX-R, tetrodotoxin-resistant; SOD2, superoxide dismutase 2; RTX, resiniferatoxin; DEGs, differentially expressed genes.

* Corresponding author. Department of Dermatology, Xiangya Hospital, Central South University, Changsha, China

E-mail address: lijj_xy@csu.edu.cn (J. Li).

¹ These authors contribute equally.

<https://doi.org/10.1016/j.redox.2022.102427>

Received 14 June 2022; Received in revised form 21 July 2022; Accepted 30 July 2022

Available online 5 August 2022

2213-2317/© 2022 The Authors. Published by Elsevier B.V. This is an open access article under the CC BY-NC-ND license (<http://creativecommons.org/licenses/by-nc-nd/4.0/>).

important role in the pathogenesis of inflammatory skin diseases, including rosacea and psoriasis [15,16]. Various risk factors induce excess ROS production in keratinocytes, which subsequently activates the proinflammatory signaling cascade, resulting in immune cell recruitment and activation across multiple skin disorders [17,18]. Several therapeutic strategies have proven beneficial for these skin disorders owing to their antioxidant characteristics [18–20].

Nav1.8, encoded by the *SCN10A* gene, is a tetrodotoxin-resistant (TTX-R) voltage-gated sodium ion channel. It is mainly expressed in sensory neurons and is closely associated with inflammatory and neuropathic pain [21]. Abnormal activation of Nav1.8 has been linked to heart rhythm disorders, cerebellar dysfunction, and peripheral neuropathy [21]. Nav1.8 generates an inward sodium current, responsible for initiating and propagating action potentials in nerves and muscles [22]. Nav1.8-specific blocking agents, including A803467, inhibit the electrophysiological properties of Nav1.8 currents and have been studied for their therapeutic implications [23,24]. Recent studies have revealed the Nav1.8 expression in non-neural cells, including keratinocytes [25]. Elevated Nav1.8 levels in the epidermal layer of the skin may contribute to pain sensitivity in complex regional pain syndrome type 1 and post-herpetic neuralgia [25,26]. However, whether and how Nav1.8 regulates the inflammatory response in keratinocytes in the skin remains unclear.

In this study, we focused on determining the role and potential mechanism of epidermal Nav1.8 in the pathogenesis of inflammatory skin disorders. We found that the expression of Nav1.8 was significantly increased in the epidermal of rosacea and psoriasis skin lesions. Functionally, the knockdown of Nav1.8 improved skin inflammation in LL37- and IMQ-induced inflammatory skin mice models. Mechanistically, Nav1.8 could induce ROS-mediated inflammatory signal in keratinocyte by binding SOD2 directly with a channel-independent mechanism. Collectively, our study sheds light on the pivotal role of Nav1.8 in skin inflammation and reveals a promising therapeutic target for inflammatory skin disorders, including rosacea and psoriasis.

2. Materials and methods

2.1. Datasets

We downloaded the gene expression data of the epidermis (GSE166388, profiled using array) from psoriasis lesions and healthy controls from the GEO database (<https://www.ncbi.nlm.nih.gov/gds/?term=>). RNA sequencing (RNAseq) data of the epidermis from rosacea lesions and healthy controls were downloaded from HRA000809 (<http://bigd.big.ac.cn/gsa-human/browse>).

2.2. Reagents

The amino acid sequence of the antimicrobial peptide LL37 was LGDFFRKSKEKIGKEFKRIVQRIKDFLRNLPRTES. LL37 was purified to >95% purity using high-performance liquid chromatography (HPLC) and synthesized by Sangon Biotech. Small interfering RNAs (siRNAs) for Nav1.8 (siNav1.8) and the negative control (NC-siRNA, siRNA with nonsense sequences) were synthesized by RiboBio (Guangzhou, China). The sequences of the probes were as follows: siNav1.8-1: CCA-CUGCCCUAAUGAUUAUTT, siNav1.8-2: GCGAGUGUGUGAUGAA-GAUTT, and NC-siRNA: TTCTCCGAACGTGTCACGTdTdT.

A803467 was purchased from Selleck Chemical (California, USA). Resiniferatoxin (RTX) was purchased from Sigma-Aldrich.

2.3. Human skin tissue samples

For rosacea, human skin tissues were collected from the central face region of patients with rosacea (n = 20) and age-matched volunteers healthy volunteers (n = 15). For psoriasis, human skin tissues were further collected from patients with psoriasis (n = 11) and healthy age-

matched volunteers (n = 11). All human skin tissues were collected from the Department of Dermatology in Xiangya Hospital, Central South University. Informed consent was obtained from all participants, and the study protocol was approved by the ethical committee of the Xiangya Hospital of Central South University (IRB number 201703212).

2.4. Experimental animals

Eight-week-old female BALB/c were used in the experiments (Slac Laboratory Animal Co., Shanghai, China). During the experiments, the mice were provided with water and food ad libitum and housed under specific pathogen-free conditions under a 12-h light/dark cycle at 24 °C. For the experiments, the mice were randomly allocated to different groups. All experiments were approved by the Ethics Committee of Xiangya Hospital, Central South University, Hunan Province, China (IRB number 201611610). All animal experiments comply the National Research Council's Guide for the Care and Use of Laboratory Animals.

2.5. Animal treatment

Various skin disorder mouse models were used in this study. To establish rosacea-like dermatitis mouse models, 40 µl of LL37 (320 µM) was intradermally injected into mice twice a day for two days. To obtain Nav1.8-knockdown mice, siNav1.8 was injected subcutaneously before the LL37 at a dose of 10 µg/day for three consecutive days in the back of mice (Fig. 2A).

A803467 was used to inhibit Nav1.8 currents. A803467 was dissolved in DMSO to reach a 50 mg/ml concentration, and 1 µl of the A803467 solution was intradermally injected along with LL37 into mice (Fig. S7). We measured the area of redness, the redness score, and the thickness of rosacea-like lesions as previously described [27].

The psoriasis-like skin inflammation mouse model was developed by applying a topical dose of 25 mg of commercially available IMQ cream (Aldara, 3 M Pharmaceuticals) on the mouse ear daily for six days. To achieve local Nav1.8 knockdown in the skin of mice, siNav1.8 was pre-injected subcutaneously in the mouse ears at doses of 5 µg/day. The first dose was administered one day before IMQ treatment and after every two days for six days (Fig. 3A). We detected erythema, scaling, and skin thickness every day.

To induce sensory nerve ablation, RTX was dissolved in methanol and injected subcutaneously into the backs of 4–5-week-old mice at doses of 30, 70, and 100 mg/kg for three consecutive days as previously described [28]. Intradermal injection of LL37 in mice at eight weeks of age was used to investigate the role of sensory fibers in the development of rosacea-like dermatitis (Fig. S3B).

All mouse experiments were repeated three times, and 5–8 mice were included in each group.

2.6. Histology and immunohistochemistry (IHC)

For histopathology, skin tissue samples were fixed, paraffin-embedded, and cut into 3-µm sections. The sections were stained with hematoxylin and eosin (H&E) and evaluated using light microscopy (OLYMPUS, Japan). For IHC, the sections were stained with a rabbit anti-Nav1.8 antibody (1:100, Sangon Biotech, D161110) or a rabbit anti-SOD2 antibody (1:100, Proteintech, 24127-1-AP) and DAB chromogen. The histopathology of the tissues was observed under a light microscope (OLYMPUS, Japan). Four representative areas of each sample were collected to evaluate the intensity of the epidermal staining on a scale of 0–4 (0 = absent, 1 = weak or low, 2 = moderate, 3 = strong, and 4 = very strong).

2.7. Cell culture and treatment

The HaCaT keratinocyte cell line was obtained from the NTCC (Laboratory of Biological Carrier Science, Beijing, China) and cultured in

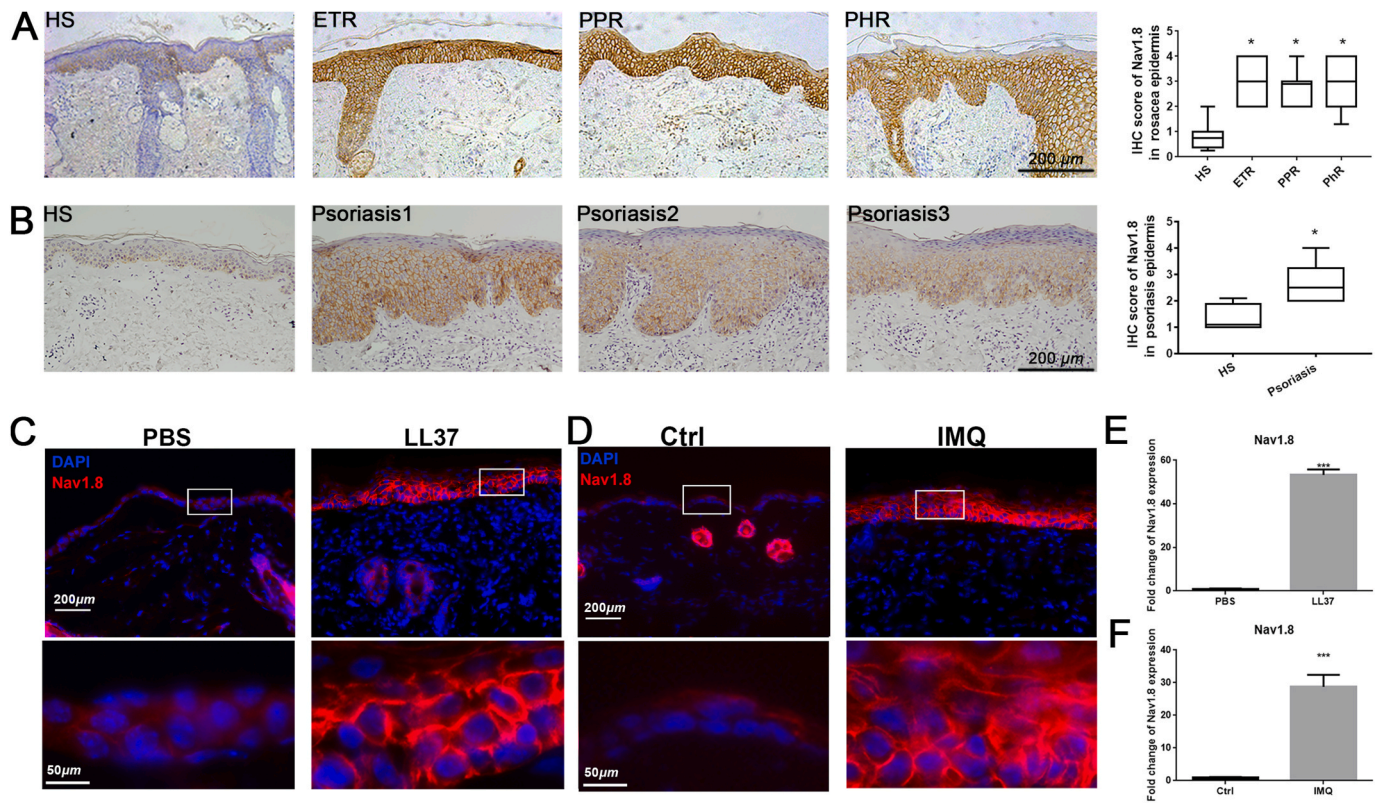


Fig. 1. Nav1.8 expression in rosacea and psoriasis. A, Immunohistochemistry (IHC) of Nav1.8 on skin tissues from HS (healthy individuals) and rosacea patients. Data represents the mean \pm SEM. * $P < 0.05$, one-way ANOVA was used. B, IHC of Nav1.8 on skin tissues from HS and psoriasis patients. Data represents the mean \pm SEM. * $p < 0.05$. Two-tailed unpaired Student's t-test was used. C, The immunofluorescence of Nav1.8 on skin tissues from PBS and LL37-induced mice. D, The immunofluorescence of Nav1.8 on skin tissues from control and IMQ-induced mice. E, qPCR analysis of Nav1.8 in skin tissues from PBS and LL37-induced mice. F, qPCR analysis of Nav1.8 in skin tissues from control and IMQ induced mice. $n = 5$ for each group, Data represents the mean \pm SEM. *** $p < 0.001$. Two-tailed unpaired Student's t-test was used.

calcium-free DMEM containing 10% fetal bovine serum, penicillin-streptomycin, and 2 mM glutamine (Invitrogen). Prior to drug treatment, the medium was replaced with DMEM containing 1.8 M calcium ions. Transfections with siRNA and plasmids were performed using Lipofectamine 2000 (Invitrogen) at a cell density of approximately 70%, according to the manufacturer's instructions. Two siRNAs (RiboBio, Guangzhou, China) were used for the Nav1.8 knockdown: si-h-Nav1.8-1 (GAGTGTGTCAGTATCATA) and si-h-Nav1.8-2 (GCTTGCTGCGCGTATTCAA). NC-siRNA (TTCTCGAAGCGTGTCACGTdTdT) was purchased from RiboBio (Guangzhou, China). For tumor necrosis factor alpha (TNF α) treatment, HaCaT cells were treated with TNF α (10 ng/ml or 100 ng/ml) for 12 h. To inhibit Nav1.8 currents, we pre-incubated cells with A803467 (100 nM) for 12 h and then treated them with TNF α for 12 h. The levels of phosphorylated proteins and associated total proteins were assessed immediately after half an hour of stimulation. In addition, mRNA levels were measured 12 h after TNF α stimulation and protein levels 24 h after TNF α stimulation. All experiments were performed at least three times (reagents not marked with the company were purchased from Thermo Fisher Scientific, USA).

2.8. RNA extraction, real-time PCR (qPCR), and RNAseq

Total RNA was extracted from mouse skin tissues and keratinocytes using TRIzol (Thermo Fisher Scientific). RNA (1 μ g) was reverse-transcribed to cDNA using the Maxima H Minus First Strand cDNA Synthesis Kit with dsDNase (Thermo Fisher Scientific). qPCR was performed on an Applied Biosystems 7500 machine (Life Technologies), and the program was set up according to the instructions of the iTaqTM Universal SYBR Green Supermix (Bio-Rad, California, USA). The delta-delta CT method was used to calculate the relative gene expression

compared to that of *GAPDH*. The expression data were further normalized to the control group for ploidy changes. The PCR primers used in this study are listed in Table 1.

For RNAseq of mouse skin samples, 1 μ g of RNA was used for the library preparation, and transcriptome sequencing was performed using Illumina HiSeq X Ten (Novogene, Beijing, China). Differentially expressed genes (DEGs) were identified with $|\log_{2}FC| > 0.5$ and $\text{adj. } p < 0.05$, using the DESeq R package. GO and KEGG enrichment analyses were performed using "clusterProfiler," "enrichplot," and "ggplot2" R packages. The PPI network was used for hub gene analysis using STRING (<https://cn.string-db.org/>) and Cytoscape (version 3.8.2).

2.9. Construction of the overexpression Nav1.8 plasmid

The plasmids used to overexpress Nav1.8 were cloned by inserting the Nav1.8 C-terminal and N-terminal (Nav1.8-C and Nav1.8-N) cDNA fragments into the pCMV-myc vector (GenePharma, Shanghai, China) using EcoRI and KpnI restriction enzymes. The empty pCMV-myc vector was used as a negative control (myc).

Nav1.8-C F (EcoRI) "3-GGGAATTCTGTACATTGCAGTGATTCTG GAGA-5"

Nav1.8-C R (KpnI) "3-GGGGTACC CTAGGGCCAGGGGCAATCA-5"

Nav1.8-N F (EcoRI) "3-GGGAATCCAATGGAgTTCCCATGGATC-5"

Nav1.8-N R (KpnI) "3-GGGGTACCCTATCATACGCCATGGTGACTA-CAG-5"

2.10. Immunoprecipitation mass spectrometry (IP-MS)

HEK293T cells were transfected with the Nav1.8-C-myc, Nav1.8-N-

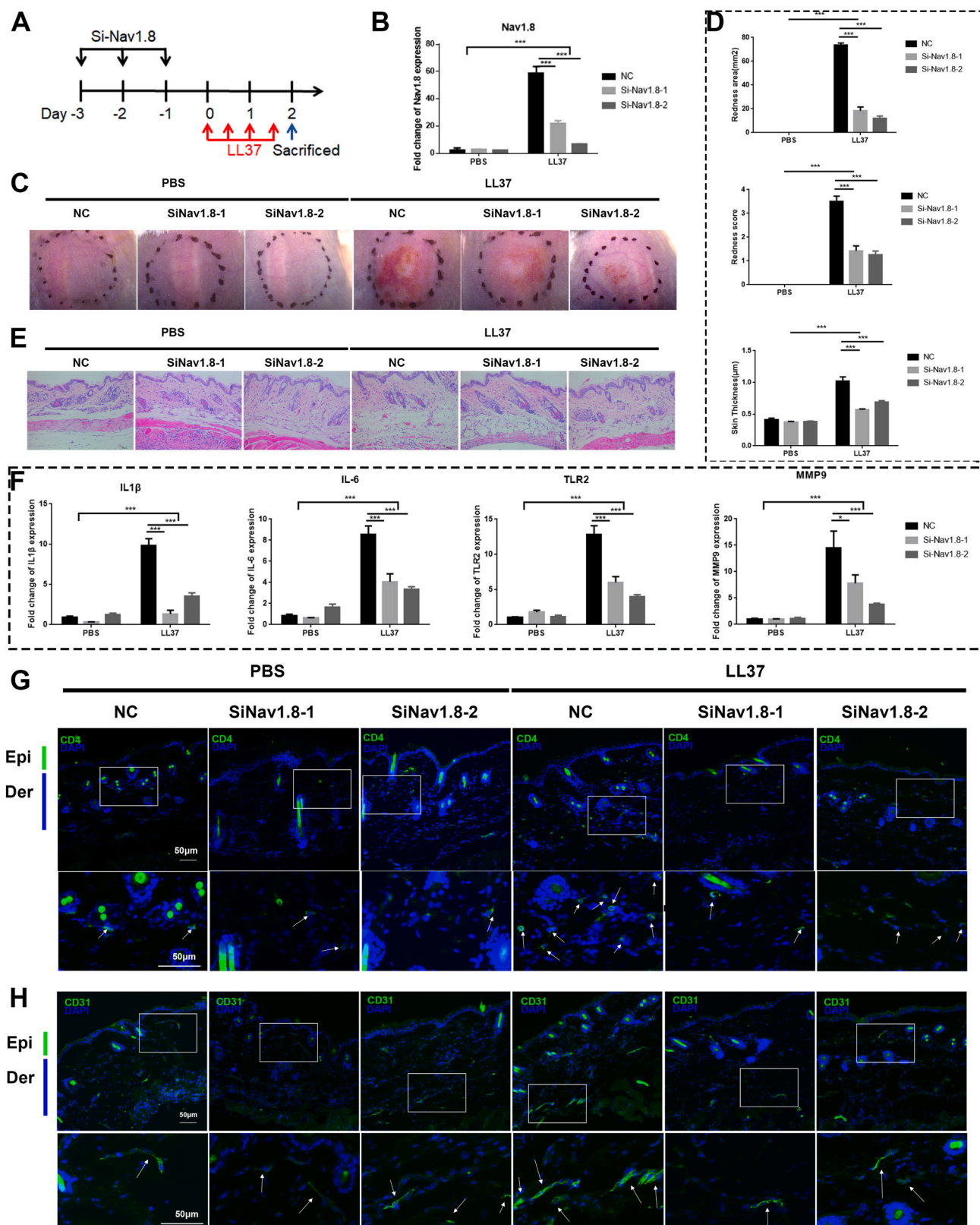
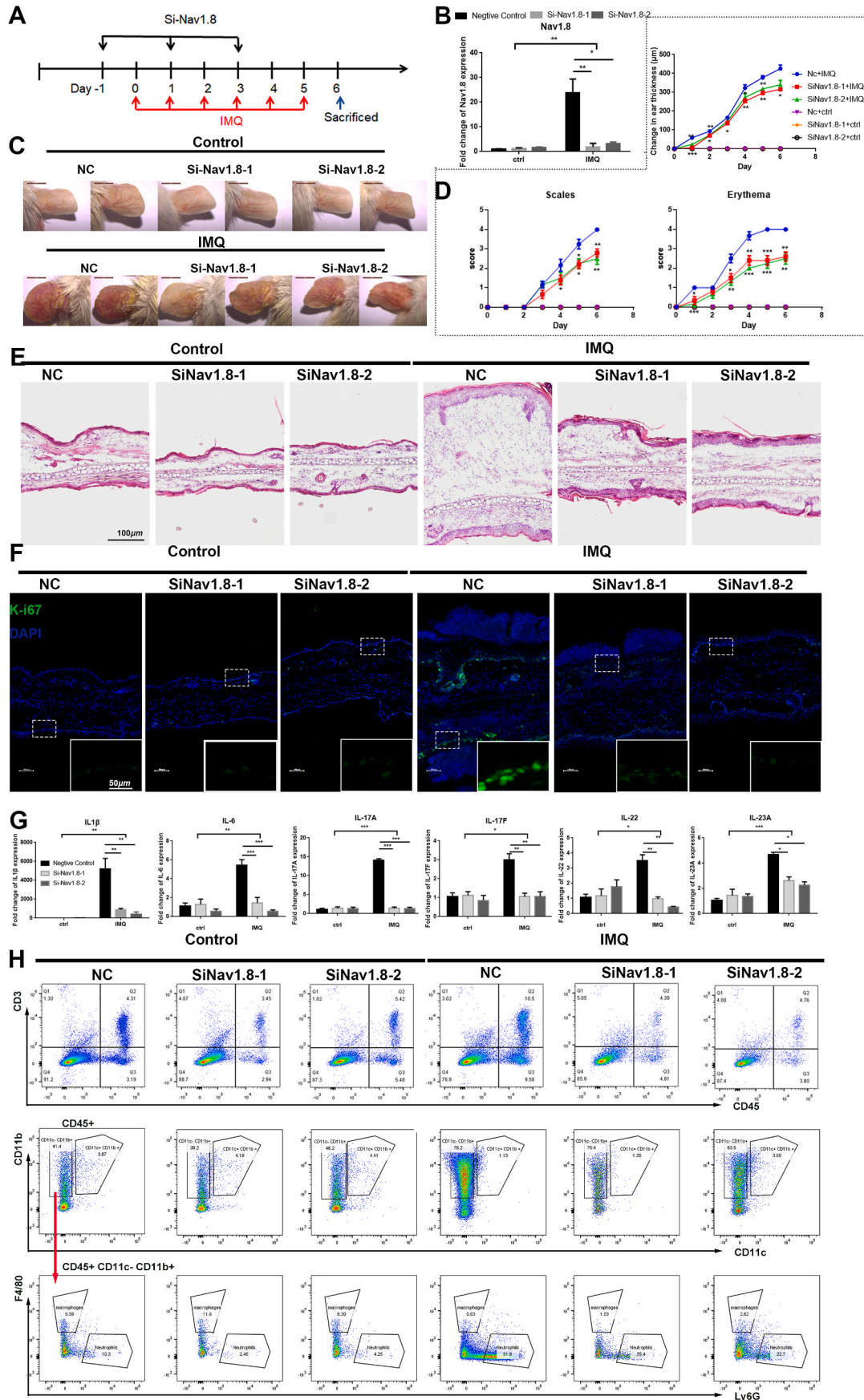


Fig. 2. Nav1.8 knockdown block rosacea-like development. A, Schematic diagram of intradermal injection of Nav1.8 for continuous 3 days before intradermal injection of LL37 in mice. B, The mRNA levels of Nav1.8 by siRNA in LL37-induced mice. C, The back skins of NC (negative control siRNA) and Nav1.8 knockdown (Nav1.8 siRNA) mice injected with LL37 or PBS. D, The reduced redness score, area of erythema and skin thickness of skin tissues in PBS/LL37-induced mice. Data represents the mean ± SEM. **p < 0.01, ***p < 0.001. 2-way ANOVA test was used. E, HE staining of lesional skin of NC and Nav1.8 knockdown mice injected with LL37 or PBS. F, The mRNA levels of IL1β, IL-6, TLR2 and MMP-9 in mice skin lesion. Data represents the mean ± SEM. **p < 0.01, ***p < 0.001. 2-way ANOVA test was used. G, The CD4⁺ T cells infiltration in mice skin lesion. H, The CD31⁺ microvascular in skin visualized by immunofluorescence. (n = 6 for each group).



(caption on next page)

Fig. 3. Knockdown Nav1.8 attenuated psoriasis-like development in mice. A, Schematic diagram of NC/Nav1.8 siRNA-injected mice treated with IMQ or control. B, The mRNA levels of Nav1.8 silenced by siRNA in the skin tissues from IMQ-induced inflammation mice. Data represents the mean \pm SEM. and * $p < 0.05$, ** $p < 0.01$, *** $p < 0.001$. 1-way ANOVA test was used. C, The ears of NC and Nav1.8 knockdown mice treated with IMQ or control. D, The erythema score, scales score and ear thickness of psoriasis-induced inflammation mice. For statistical analysis, siRNA-IMQ group was compared with NC-IMQ group, * $p < 0.05$, ** $p < 0.01$, *** $p < 0.001$. 1-way ANOVA test was used. E, HE staining of lesional skin of WT and Nav1.8 knockdown mice treated with IMQ. F, The Ki67 expression visualized by immunofluorescence. G, The mRNA levels of IL1 β , IL-6, IL17-A, IL-17F, IL-22, IL23A in IMQ-induced inflammation mice. H, The flow cytometry analysis revealed the immune cells infiltration in the skin lesion of IMQ-induced inflammation mice.

Table 1
List of primers used for Real-time PCR.

Target gene	Forward primers	Reverse primers
Mouse GAPDH	AGGTCGGTGTGAACGGATTG	TGTAGACCATGTAGTTGAGGTCA
Mouse Nav1.8	AATCAGAGCGAGGAGAAGACG	CTAGTGAGCTAAGGATCGCAGA
Mouse IL1 β	GCAACTGTCTCTGAACCTCACT	ATCTTTTGGGGTCCGTCACACT
Mouse IL6	TAGTCCTTCTACCCCAATTTCC	TTGGTCTTAGCCACTCCTTC
Mouse TLR2	TCTAAAGTCGATCCCGACAT	CTACGGGCAAGTGGTAAAAC
Mouse MMP9	CTGGACAGCCAGACACTAAAG	CTCGCGCAAGTCTTCAGAG
Mouse TNF- α	CTGAACTTCGGGGTATCGG	GGCTTGTCACTCGAAATTTGAGA
Mouse IL17A	TTTAACTCCCTGGCGCAAAA	CTTCCCTCCGATTGACAC
Mouse IL17F	TGCTACTGTTGATGTTGGGAC	CAGAAATGCCCTGGTTTTGGT
Mouse IL22	ATGAGTTTTCCCTTATGGGGAC	GCTGGAAGTTGGACACCTCAA
Mouse IL23A	AGCCCACTCCTCAGCCAGAG	CGCTGCCACTGCTACTAGAAC
Human GAPDH	TGTTGCCATCAATGACCCTT	CTCCACGACGTACTCAGCG
Human IL6	CCTGAACCTTCCAAGATGGC	TTCACGAGCAAGTCTCCTCA
Human IL1 β	AGCTACGAATCTCCGACCAC	CGTTATCCCATGTGTGGAAGAA

myc, and pCMV-myc vectors. Twenty-four hours after transfection, cell lysates were collected and pre-cleared with appropriate control IgG and Protein A/G PLUS-Agarose beads (Santa Cruz Biotechnology). The beads were removed and incubated with Protein A/G PLUS-Agarose beads and an anti-myc antibody (1:1,000, Proteintech, 60003-2-Ig) overnight. The protein was then digested with trypsin. The peptides were separated using an Ultimate 3000 RSLCnano system and analyzed using the Q Exactive (Thermo Fisher Scientific, San Jose, CA, USA). Proteome discoverer version 1.4 (PD1.4; Thermo Fisher Scientific) and the search algorithm Mascot were used for protein identification.

2.11. Immunofluorescence (IF) analysis

Human and mouse skin lesions and mouse dorsal root ganglions (DRGs) were embedded in O.C.T. (Tissue Tek). Tissue sections (8 μ m) and HaCaT cells were fixed in 4% paraformaldehyde and blocked with a blocking solution (5% NDS(Normal Donkey Serum), 0.3% Triton X-100 in PBS). Primary antibodies were incubated overnight at 4 $^{\circ}$ C. The following primary antibodies were used in this study: rabbit anti-Nav1.8 (1:200, Sangon Biotech, D161110), anti-Nav1.8 (1:100, Alomone Lab, ASC-016), rat anti-CD4 (1:100, eBioscience, 14-0042-85), rat anti-CD31 (1:100, BD Biosciences, 558736), mouse anti-SOD2 (1:200, Santa Cruz, sc-137254), rabbit anti-SOD2 (1:200, Proteintech, 24127-1-AP), rabbit anti-IL1 β (1:200, Proteintech, 16806-1-AP), and mouse anti-IL6 (1:200, Proteintech, 66146-1-Ig). Alexa Fluor 488- or 594-coupled secondary antibodies (1:500, Thermo Fisher Scientific) were incubated for 1 h at room temperature (RT). Sections were stained with 4',6-diamidino-2-phenylindole (DAPI). All photographs were captured using a Zeiss Axio Scope A1 microscope (Zeiss, Germany).

2.12. Mitochondrial fluorescence

Fifty microliters of lyophilized MitoTracker[®] Red CMXRos (Cell Signaling Technology, 9082) were dissolved in DMSO to a 1 mM stock solution. The stock solution was diluted directly in the cell culture medium to a concentration of 50 nM, and the cells were incubated for 30 min at 37 $^{\circ}$ C. After incubation, the cells were fixed in pre-cooled methanol for 15 min at -20 $^{\circ}$ C and washed with PBS for 15 min. The samples were then used for immunofluorescent staining.

2.13. Mitochondrial protein extraction

Cytosolic and mitochondrial proteins were isolated according to the method described by Demet Candas et al. [29]. Briefly, cells were collected and homogenized in ice-cold IBC buffer, and centrifuged at 600 \times g for 10 min at 4 $^{\circ}$ C. The supernatant was collected and centrifuged at 7000 \times g for 10 min at 4 $^{\circ}$ C. At this point, cytoplasmic lysine was present in the supernatant and mitochondria in the precipitate. The supernatant was removed, and the precipitate was resuspended in RIPA buffer (Thermo Fisher Scientific) containing a protease inhibitor (Thermo Fisher Scientific) to lyse the mitochondrial proteins. Total protein extraction was done by direct lysing the cells in RIPA buffer.

2.14. Immunoblotting

Protein concentrations were determined using the bicinchoninic acid assay (Thermo Fisher Scientific). Proteins were separated by sodium dodecyl sulfate-polyacrylamide gel electrophoresis and transferred to polyvinylidene fluoride or polyvinylidene difluoride membranes. The membranes were blocked with 5% skim milk for 1 h at RT and then incubated with the primary antibody overnight at 4 $^{\circ}$ C. The following primary antibodies were used: rabbit anti-p38 (1:1,000, Abcam, ab170099), rabbit anti-p38-phospho-t180 (1:1,000, Abcam, ab178867), rabbit anti-p65 (1:1,000, Cell Signaling, #8242s), rabbit anti-phospho-p65 (1:1,000, Cell Signaling, #3033s), rabbit anti-Nav1.8 (1:1,000, Alomone Lab, Israel), rabbit anti-SOD2 (1:2,000, Proteintech, 24127-1-AP), rabbit anti-SOD2/mnsod-acetyl-k68 (1:1,000, Abcam, ab137037), mouse anti-Myc (1:1,000, Proteintech, 60003-2-Ig), mouse anti- β -actin (1:5,000, Proteintech, 66009-1-Ig), mouse anti- β -Tubulin (1:5,000, Proteintech, 10094-1-AP), and rabbit anti-GAPDH (1:5,000, Bioworld, AP0066). The next day, the samples were incubated with an HRP-coupled secondary antibody (Santa Cruz Biotechnology). Immunoreactive strips were visualized on a ChemiDoc TM using HRP substrate (Luminata, Millipore) on the XRS + system (Bio-Rad). The expression levels of β -actin, β -tubulin, and GAPDH were used as controls.

2.15. Co-immunoprecipitation (Co-IP) assay

The interaction between Nav1.8 and SOD2 was verified by Co-IP analysis. Cells were lysed using IP lysis buffer (Beyotime, Shanghai,

China) and incubated with specific antibodies (rabbit anti-Nav1.8 (Alomone Lab, Israel), rabbit anti-SOD2 (Proteintech, 24127-1-AP) and mouse anti-Myc (Proteintech, 60003-2-Ig) or IgG overnight at 4 °C. The complexes were then incubated with protein A/G beads (Santa Cruz Biotechnology, Santa Cruz, CA, USA) and analyzed by protein blotting.

2.16. Flow cytometry

To isolate single cells, tissue samples were minced and incubated in DMEM containing collagenase, type 4 (2 mg/ml, Worthington Biochemical, LS004188) and dispase II (1 mg/ml, SIGMA, D4693) for 100 min, with shaking at 37 °C. The digestion was stopped with DMEM containing 10% FBS and filtered through a 70- μ m cell filter (BD). The cells were then diluted 1:100 with Zombie Aqua™ dye in PBS, resuspended, and incubated for 15 min at RT in the dark. The single-cell suspension was incubated with Fc Block for 15 min at 4 °C. After washing, a mixture of cell surface antibodies was added, followed by incubation for an additional 30 min at 4 °C in the dark. We used the following antibodies: anti-CD45-FITC (eBioscience, California USA), anti-CD3-PerCP-Cy5.5 (eBioscience, California, USA), anti-CD11b-Pacific Blue (eBioscience, California, USA), anti-CD11c-PE-Cy7 (eBioscience, California, USA), anti-F4/80-PE (eBioscience, California, USA), and anti-ly6G-PerCP-Cy5.5 (eBioscience, California, USA). Cells were then fixed and permeabilized using the BD Cytotfix/Cytoperm kit (BD Biosciences, San Jose, CA, USA) according to the manufacturer's instructions and detected using flow cytometry (FACSCalibur, BD, San Jose, CA).

2.17. ROS detection

Intracellular ROS levels were detected using the Reactive Oxygen Species assay kit (DCFH-DA, Beyotime Institute of Biotechnology). The DCFH-DA was diluted 1:1000 in serum-free medium to a final concentration of 10 μ M. The diluted DCFH-DA was added to the culture dish to adequately cover the cells, and the culture was incubated for 20 min in a 37 °C cell incubator. Cells were washed three times with serum-free medium to sufficiently remove the extra DCFH-DA that had not entered the cells. The cells were collected, and the fluorescence intensity was measured at an excitation wavelength of 488 nm and an emission wavelength of 525 nm using a Zeiss Axio Scope A1 (Zeiss, Germany). For mitochondrial ROS scavenging, cells were pretreated with MitoTEMPO (10 μ M, SML0737, Sigma-Aldrich) for 24 h and transfected with Nav1.8-C. Sixteen hours later, cells were collected for ROS detection and qPCR analysis.

2.18. Dihydroethidium (DHE) staining

Superoxide anion levels and ROS production in frozen sections/cells were evaluated using DHE staining. The frozen tissue sections (8 μ m) were incubated with 5 μ mol/l DHE (Beyotime, China) in PBS at 37 °C for 30 min in the dark. The sections were washed three times with PBS for 5 min to remove extracellular DHE. All photographs were captured using a Zeiss Axio Scope A1 microscope (Zeiss, Germany).

2.19. SOD assay

After the overexpression or knockdown of Nav1.8 in cells by transfection with siRNA or Nav1.8 plasmid, cells were stimulated with 10 ng/ml TNF α for 24 h. The total SOD activity was subsequently measured using a water-soluble tetrazolium salt (WST-8) kit (total superoxide dismutase assay kit with WST-8, Beyotime). One unit of SOD activity was defined as the amount of enzyme that reduced WST-8 methanogen formation by 50%.

2.20. Statistical analyses

Statistical analyses were performed using GraphPad 7.0. Data are shown as the mean \pm SEM. Normal distribution and similar variance between groups were analyzed. Differences between groups were compared using the Student's t-test. One-way or two-way analysis of variance (ANOVA) with a relevant post hoc test was used for multiple comparisons (* p < 0.05, ** p < 0.01, *** p < 0.001). The two-tailed Mann-Whitney U test was performed for data that were not normally distributed or if the variances of the two groups were unequal.

3. Results

3.1. Nav1.8 expression in the epidermis is increased in rosacea and psoriasis

First, we evaluated the Nav1.8 expression levels in the skin lesions of patients with rosacea and psoriasis. The results showed that the mRNA levels of Nav1.8 were significantly increased in rosacea and psoriasis skin lesions compared to healthy controls (Fig. S1A). To confirm this finding at the protein level, we performed IHC to detect Nav1.8 expression in skin tissues from patients with rosacea or psoriasis and healthy individuals. As shown in Fig. 1A and B, Nav1.8 was mainly expressed in the epidermis of normal skin, and its expression was evidently increased in the skin lesions from patients with rosacea or psoriasis. In addition, we detected Nav1.8 expression in two classic skin inflammation mouse models, the LL37-induced rosacea-like skin inflammation model and the IMQ-induced psoriasis-like skin inflammation model. Consistent with the results in human skin lesions, the skin lesions from LL37-induced mice and IMQ-induced mice showed a significant upregulation in Nav1.8 expression in the epidermis compared to normal skin tissue (Fig. 1C and D). qPCR analysis of full-thickness skin showed that the mRNA levels of Nav1.8 were dramatically upregulated in skin lesions of both mouse models (Fig. 1E and F). Together, these data demonstrate that Nav1.8 expression is upregulated in the epidermis of inflammatory skin diseases, including rosacea and psoriasis.

3.2. Nav1.8 is essential for LL37-induced skin inflammation in mice

To dissect the role of Nav1.8 in rosacea, we silenced Nav1.8 in the skin of the LL37-induced mice (Fig. 2A). qPCR and IF staining results showed that siNav1.8 reduced the expression of Nav1.8 in LL37-induced inflammatory skin lesions (Fig. 2B and Fig. S2B). Nav1.8 knockdown reduced rosacea-like features, including a lower redness score, area of erythema, and a decrease in skin thickness, compared with these features in the NC mice after LL37 injection (Fig. 2C–D and Fig. S2A). Histological analysis revealed that inflammatory cell infiltration was significantly reduced in the Nav1.8-knockdown mice (Fig. 2E and Fig. S2C). The levels of disease-characteristic factors, including IL6, TLR2, MMP-9, and IL1 β , were dramatically reduced in the Nav1.8-knockdown mice (Fig. 2F). Notably, and in agreement with these findings, the infiltration of CD4⁺ T cells and the number of CD31⁺ vessels were significantly reduced in the Nav1.8-knockdown group compared to the NC group (Fig. 2G and H). These results indicate that Nav1.8 is essential for LL37-induced skin inflammation.

Given the essential role of Nav1.8 in sensory nerve and nerve-mediated inflammatory regulation, we used RTX-treated mice with sensory nerve ablation to detect the potential role of the Nav1.8⁺ sensory nerve in the LL37-induced mice. The results showed that RTX treatment did not affect the epidermal Nav1.8 expression and rosacea-like phenotype (Figs. S3A–F), indicating that sensory nerves did not affect LL37-induced skin inflammation in mice.

3.3. Nav1.8 is involved in IMQ-induced skin inflammation in mice

We further used the IMQ-induced mice to investigate the role of

epidermal Nav1.8 in psoriasis pathogenesis (Fig. 3A). The qPCR and IF staining results showed that siNav1.8 reduced the expression of Nav1.8 in the epidermis of IMQ-induced inflammatory skin lesions (Fig. 3B and Fig. S4A). As shown in Fig. 3C and D, Nav1.8 knockdown reduced the scaliness, erythema, and thickness of psoriasiform skin lesions. Histological analysis revealed that severe dermatitis, including pronounced acanthosis, parakeratosis, and the number of dermis-infiltrating cells, in IMQ-induced psoriasiform skin was improved in the Nav1.8-knockdown mice (Fig. 3E and Figs. S4B and D). Keratinocyte proliferation was also reduced in Nav1.8-knockdown mice (Fig. 3F). The levels of proinflammatory cytokines (IL1 β , IL6, IL17a, IL17f, IL22, and IL23a) and infiltration of immune cells, especially neutrophils, were significantly decreased by Nav1.8 knockdown in psoriasiform skin lesions (Fig. 3G and H). Moreover, the spleen in Nav1.8-knockdown mice was reduced in size (Fig. S4C). Taken together, these results demonstrate the important role of epidermal Nav1.8 in the pathogenesis of psoriasis.

3.4. Nav1.8 promotes the progression of inflammatory skin disease by regulating cytokine expression in keratinocytes

To reveal the potential mechanism by which Nav1.8 promotes skin inflammation, we performed RNAseq to identify genes that were abnormally expressed in rosacea-like skin lesions and regulated by Nav1.8. Most of the DEGs induced by LL37 were reversed by the Nav1.8 knockdown. The results showed that 2500 genes were upregulated in response to LL37 stimulation (Fig. 4A and Fig. S5A), and 2390 of these were rescued by siNav1.8. Many of these genes were enriched in cytokine- and leukocyte migration-related biological processes (Fig. 4C). A total of 2600 genes were downregulated in response to LL37 stimulation (Fig. 4B and Fig. S5A), of which 2240 were rescued by siNav1.8. The effect of the siNav1.8 rescue on LL37-induced expression can be observed in the heatmap of DEGs (Fig. S5). Previous studies have reported abnormal expression of genes related to T-cell activation, Th1/Th17 polarization, and macrophage and neutrophil activation in rosacea tissues [30]. Consistent with this result, our RNAseq results showed that the genes related to T-cell activation, Th1/Th17 differentiation, macrophage and neutrophil activation were significantly dysregulated in LL37-induced inflammatory skin lesions, and these effects were ameliorated by Nav1.8 knockdown (Fig. 4D). Previous studies have reported an important role of keratinocyte-secreted cytokines in immune cells infiltration in various inflammatory skin diseases [31]. Among the above genes, IL6 and IL1 β were identified as hub genes using PPI network analysis (Fig. 4E). These genes are involved in the regulation of the top five biological processes in rosacea progression (Fig. 4C). Moreover, the upregulation of IL6 and IL1 β in keratinocytes was also verified in previous epidermal transcriptome data of rosacea and psoriasis (Fig. 4F). This indicates that epidermal IL6 and IL1 β may play a key role in Nav1.8-mediated skin inflammation, thereby contributing to the pathogenesis of inflammatory skin disorders. Consistent with this speculation, the mRNA levels of IL1 β and IL6 were increased by LL37 and IMQ and attenuated by Nav1.8 knockdown (Figs. 2F and 3G). IF results revealed that IL1 β and IL6 expression was increased in the epidermis of LL37- and IMQ-induced inflammatory skin lesions and was attenuated by Nav1.8 knockdown (Fig. 4G and H). Collectively, these findings suggest that Nav1.8 is vital to skin inflammation partly by regulating IL1 β and IL6 production in keratinocytes.

3.5. Nav1.8 induced the pro-inflammatory cytokines production and ROS accumulation in keratinocytes

TNF α is a well-known cytokine that promotes skin inflammation in rosacea and psoriasis. We, therefore, addressed the role of Nav1.8 in TNF α -induced inflammation in keratinocytes. We found that TNF α induced Nav1.8 expression in keratinocytes, which was decreased by Nav1.8 siRNAs (Fig. 5A and Fig. S6A). Moreover, Nav1.8 knockdown suppressed TNF α -induced expression of IL1 β and IL6 (Fig. 5B). The NF-

κ B and MAPK pathways participate in the TNF α -induced production of pro-inflammatory cytokines in keratinocytes [19]. Here, phosphorylated p38 and p65 levels were increased by TNF α stimulation and reduced by Nav1.8 knockdown (Fig. 5C and Fig. S6B). Nav1.8, a voltage-gated ion channel, performs its channel function mainly by opening/closing the channel structure. Here, we used A803467, a Nav1.8-specific blocker, to inhibit the electrophysiological properties of Nav1.8 currents [24]. However, A-80367 treatment did not affect IL1 β or IL6 expression (Fig. 5D). Moreover, the functional inhibition of Nav1.8 by A803467 did not affect the LL37-induced rosacea-like inflammation (Fig. S7). These results indicate that Nav1.8 is involved in producing pro-inflammatory cytokines independent of its conduction role.

Previous studies have revealed the contribution of ROS in rosacea and psoriasis development [32,33]. ROS-activated proinflammatory signals in keratinocytes play a crucial role in immunoregulating inflammatory skin diseases. Therefore, we investigated the effects of Nav1.8 on ROS accumulation in LL37- and IMQ-induced mice and TNF α -stimulated keratinocytes. In vivo, DHE staining results showed that ROS levels were significantly increased in the keratinocytes of LL37- and IMQ-induced skin lesions and decreased in Nav1.8-knockdown mice (Fig. 5F). In vitro, ROS levels were increased by TNF α stimulation, which was attenuated by siNav1.8 treatment (Fig. 5E and Figs. S8A and B). However, TNF α -induced ROS accumulation was not affected by the A803467 treatment (Fig. 5E). Therefore, we speculated that upregulated Nav1.8 induced the production of proinflammatory cytokines in keratinocytes partly by promoting ROS accumulation.

3.6. The Nav1.8 regulates cytokines production and ROS accumulation by targeting SOD2 directly

As ion channel proteins, cytosolic N- and C-terminals are essential for the localization and function of Nav1.8 [34]. To reveal the potential mechanism by which Nav1.8 regulates inflammation in keratinocytes, we cloned Nav1.8-N and Nav1.8-C into the myc plasmid to identify their interaction with proteins using IP-MS. In total, 33 and 69 proteins were identified to interact with the Nav1.8-N and Nav1.8-C groups, respectively, compared to the empty vector plasmid. GO analysis showed that proteins (such as SOD2, GSTP1, PRDX1) related to antioxidant activity, peroxidase activity, and oxidoreductase activity were among the proteins potentially interacting with the Nav1.8-C (Fig. 5I).

Considering the important role of ROS in skin inflammation, we hypothesized that Nav1.8-C affects ROS levels by binding to these proteins, thereby regulating inflammation. Next, we examined the role of Nav1.8-C in ROS accumulation and inflammation in HaCaT cells. As shown in Fig. 5H, Nav1.8-C induced ROS accumulation and IL1 β and IL6 expression in HaCaT cells. Next, a specific mtROS-targeted antioxidant, MitoTempo, was used to reduce the ROS levels in keratinocytes. We found that the mtROS scavenger significantly reduced Nav1.8-C-induced ROS accumulation and increased IL1 β and IL6 expression in keratinocytes (Fig. 5H).

Antioxidant enzymes play a key role in the regulation of cellular ROS. We, therefore, selected the antioxidant enzyme SOD2 for further analysis and verified the interaction between Nav1.8 and SOD2 using Co-IP assay. By transfecting the Nav1.8-C, Nav1.8-N, and myc-vector into keratinocytes, exogenous Co-IP revealed the interaction of SOD2 with Nav1.8-C (Fig. 5J). This result was also confirmed by endogenous Co-IP in the DRG cells (Fig. 5K). Moreover, IF showed that SOD2 and Nav1.8 co-localized in human skin and DRG cells (Fig. S9). Collectively, these results indicate that Nav1.8-C interacts with SOD2 to induce ROS accumulation and subsequently leads to cytokine production in keratinocytes.

3.7. Nav1.8 affects SOD2 translocation into mitochondria

Since Nav1.8 interacted with SOD2, we aimed to determine whether

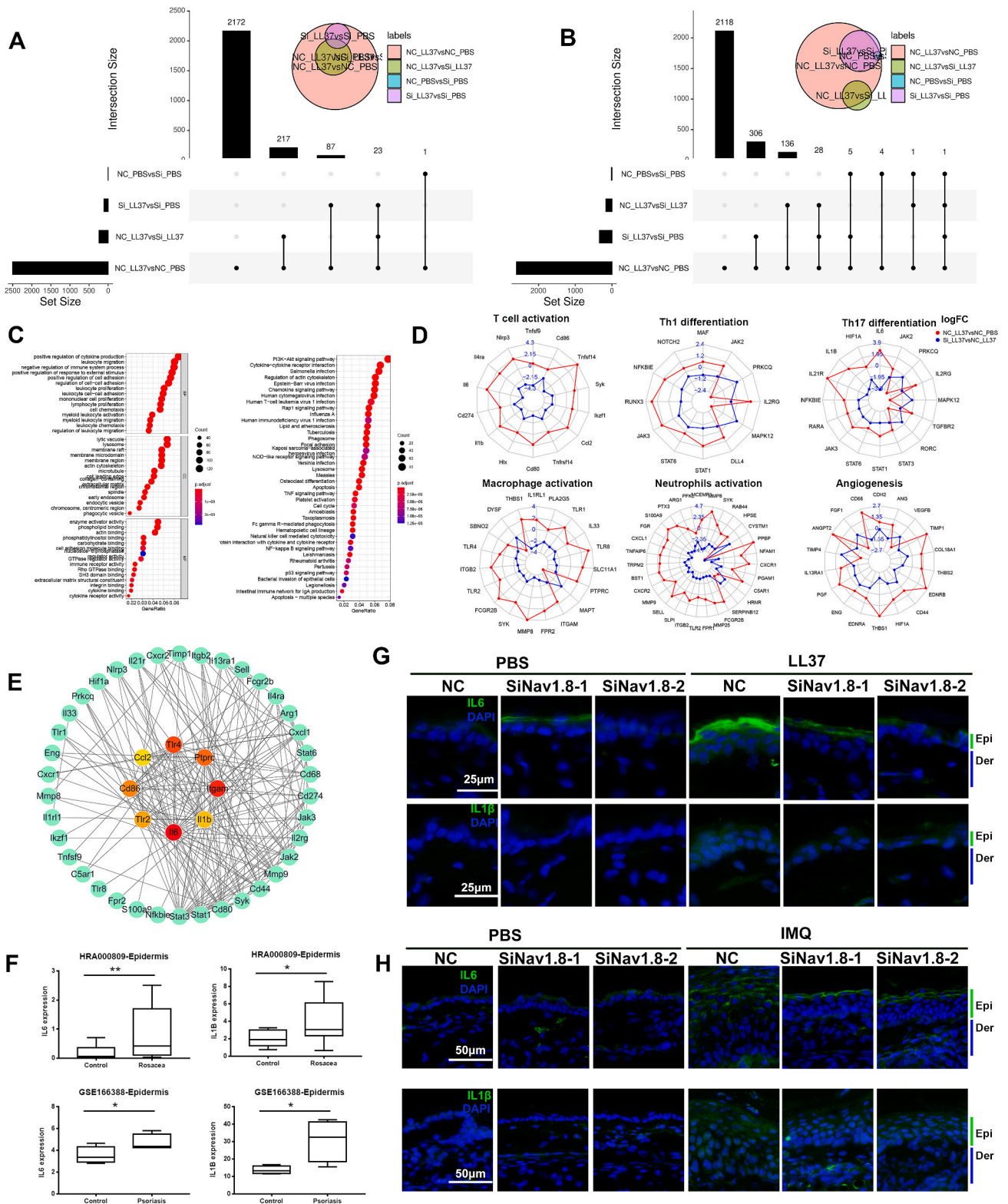


Fig. 4. Nav1.8 promoted the progression inflammatory skin disease by regulating cytokines expression in keratinocytes. **A**, The upregulated genes in NC_LL37 group compared to NC_PBS group. **B**, The downregulated genes in NC_LL37 group which were attenuated by Nav1.8 siRNA. **C**, The GO and KEGG enrichment analysis of the 2390 genes upregulated in NC_LL37 group which were attenuated by Nav1.8 siRNA. **D**, The T cell activation, Th1/Th17 differentiation, macrophage and neutrophils activation-related genes expression in NC_LL37 group compared to NC_PBS group and in Si_LL37 group compared to NC_LL37 group. **E**, PPI network analysis revealed the hub genes of these immune-cell related genes. **F**, The IL1β and IL6 expression in the keratinocytes of rosacea and psoriasis from HRA000809 and GSE166388 datasets. Data represents the mean ± SEM. * $p < 0.05$, ** $p < 0.01$. Two-tailed unpaired Student's t-test was used. **G**, The IL1β and IL6 expression in skin lesion from NC and Nav1.8 knockdown mice injected with LL37 or PBS. **H**, The IL1β and IL6 expression in skin lesion from NC and Nav1.8 knockdown mice treated with IMQ or control visualized by immunofluorescence.

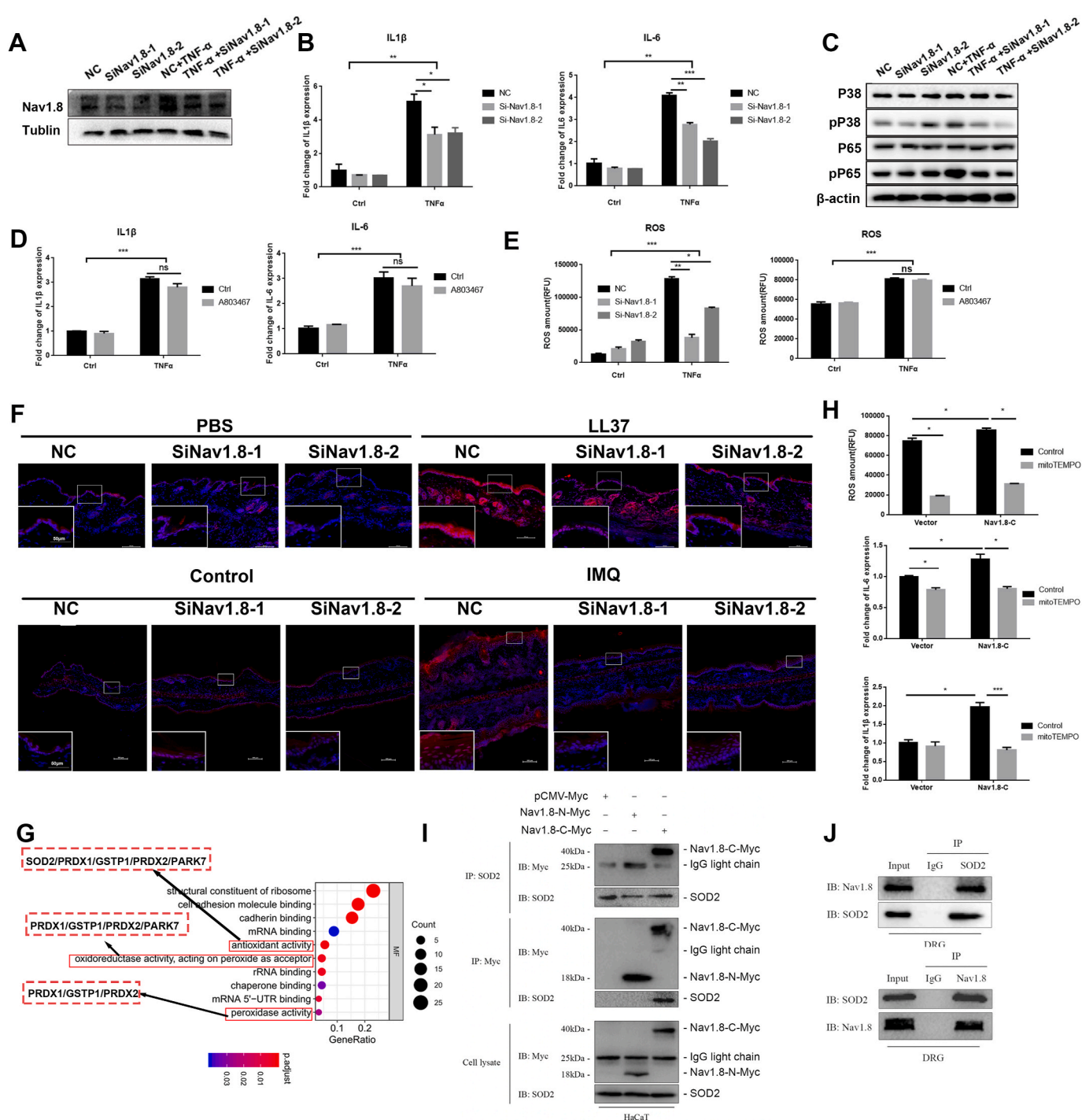


Fig. 5. Nav1.8 induced ROS accumulation in keratinocyte by interacting with SOD2 directly. **A**, Nav1.8 expression in NC and Nav1.8 knockdown keratinocyte treated with TNF α . **B**, IL-1 β and IL-6 expression in NC and Nav1.8 knockdown keratinocyte treated with TNF α . **C**, P38, p-P38, P65, p-P65 expression in control and Nav1.8 knockdown keratinocyte treated with TNF α . **D**, IL-1 β and IL-6 expression in control and A-803467-treated keratinocyte stimulated with TNF α . **E**, The ROS levels of keratinocyte treated with TNF α and Nav1.8 siRNA or A803467. **F**, The DHE staining of skin lesion from NC and Nav1.8 knockdown mice treated with IMQ or control or PBS or LL37. **G**, GO enrichment analysis of potential interaction proteins of Nav1.8 C-terminal. **H**, The ROS levels of and mRNA levels of IL-1 β and IL-6 in Nav1.8-C overexpressed keratinocyte treated with mitoTEMPO. **I**, Co-IP revealed the interaction between Nav1.8-C and SOD2 in keratinocytes. **J**, The endogenous Co-IP revealed the interaction between Nav1.8 and SOD2 in DRG (Dorsal root ganglion). Data represents the mean \pm SEM. and * p < 0.05, ** p < 0.01, *** p < 0.001. 2-way ANOVA test was used.

Nav1.8 regulates SOD2 expression. We found that neither a knockdown nor overexpression of Nav1.8 affected SOD2 expression (Fig. 6A and E, Fig. S10A). We next tested whether Nav1.8 affected the SOD2 function. To this end, we tested the SOD2 activity using a SOD assay. We found that the Nav1.8 knockdown increased SOD2 activity whereas Nav1.8-C

and TNF α decreased SOD2 activity in keratinocytes (Fig. 6B). Moreover, SOD2 activity was not affected by the A-80367 treatment (Fig. 6B).

SOD2 only plays a role in ROS clearance when it is translocated from the cytoplasm into the mitochondria [13]. We hypothesized that Nav1.8 could affect the translocation of SOD2 into the mitochondria. To verify

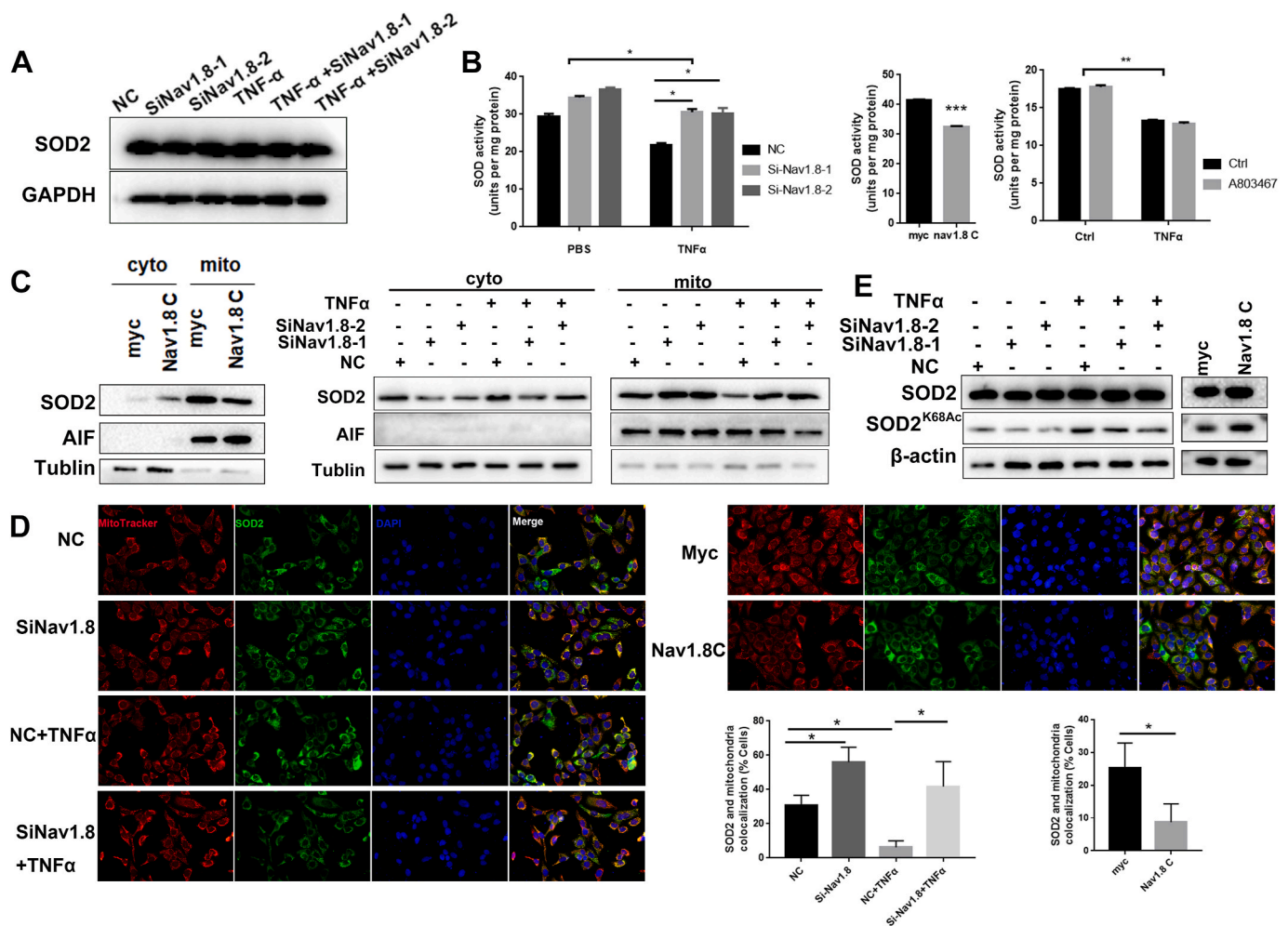


Fig. 6. Nav1.8 affects the translocation and acetylation levels of SOD2. A, SOD2 expression in NC and Nav1.8 knockdown keratinocytes treated with TNF α . B, SOD2 activity of NC and Nav1.8 knockdown keratinocyte treated with TNF α , or SOD2 activity of Nav1.8C-overexpressed keratinocyte cells, or SOD2 activity of A803467 treated keratinocyte cells. C, Western blots revealed the effects of Nav1.8-siRNA, Nav1.8-C, or TNF α on the levels of SOD2 in the cytosolic and mitochondrial fractions. D, The immunofluorescence revealed the mitochondrial SOD2 localization. E, Western blots revealed the effects of Nav1.8-siRNA, Nav1.8-C, or TNF α on the levels of SOD2 K68 acetylation.

this hypothesis, mitochondrial and cytoplasmic proteins were extracted after Nav1.8-C overexpression or Nav1.8 knockdown. Nav1.8-C overexpression induced the accumulation of SOD2 in the cytoplasm, and Nav1.8 knockdown resulted in the accumulation of SOD2 in the mitochondria (Fig. 6C). IF analysis showed that the co-localization of SOD2 with mitochondria was significantly increased in the Nav1.8-C group but decreased in the Nav1.8-knockdown groups (Fig. 6D). Because the deacetylation of SOD2 is essential for SOD2 activity, we next determined whether Nav1.8 affects the acetylation levels of SOD2. As expected, acetylation of lysine 68 (SOD2^{K68Ac}) was increased by Nav1.8-C and decreased by siNav1.8 in keratinocytes (Fig. 6E and Fig. S10B). The above results indicate that Nav1.8 reduces SOD2 activity by reducing mitochondrial transport and increasing the acetylation levels of SOD2 in keratinocytes.

4. Discussion

Rosacea and psoriasis are common inflammatory skin disorders with high global prevalence [1,35]. Despite numerous studies demonstrating the important role of disordered keratinocyte signaling in the pathogenesis of rosacea and psoriasis, the underlying pathological mechanisms remain poorly defined. In this study, we concluded that Nav1.8 is upregulated in the epidermis of rosacea and psoriasis, and Nav1.8 knockdown attenuated rosacea-like and psoriasis-like skin inflammation

in a mouse model. Mechanistically, Nav1.8 induces ROS-mediated proinflammatory signaling in keratinocytes by interacting with SOD2 to limit its mitochondrial translocation and deacetylation.

Nav1.8, a member of the voltage-gated sodium channel family, is predominantly expressed in excitatory cells, including cardiomyocytes and nerve cells. Nav1.8 in the atria is an essential contributor to the late Na⁺ current (I_{NaL}), which impacts atrial arrhythmogenesis directly [23]. A common gain-of-function variant is associated with heart block and ventricular arrhythmias [36]. Nav1.8 contributes to driving action potential conduction in neurons and is involved in pain conditions and sensory neuron-driven immune regulation [28,37]. Although several studies have demonstrated the important role of sensory neurons in the pathogenesis of rosacea [38], nerve ablation and the specific inhibition of Nav1.8 current by A803467 *did not* influence LL37-induced skin inflammation in this study. For other skin inflammations, including psoriasis [28] and HSV-1 infection [39], it should be noted that sensory neuron ablation reduced skin inflammation from day three post-IMQ treatment [28] and four days post-HSV-1 infection [39], indicating that the neurological effect on immunity is only detectable after a few days. Several studies have shown Nav1.8 expression in non-excitatory cells, including sperm [40], glia [41], and keratinocytes [25]. Dysfunctional keratinocytes play a pivotal role in the development and maintenance of inflammation in inflammatory skin disorders [42]. Here, we found that Nav1.8 expression increased in the epidermis of

individuals with rosacea and psoriasis, and its knockdown reduced the inflammatory response after two days in IMQ- and LL37-induced mice. This finding suggests that Nav1.8 in epidermal keratinocytes may initiate inflammation and the development of rosacea and psoriasis.

Impaired inflammatory signals in keratinocytes are essential for driving skin inflammation in rosacea and psoriasis [5,43]. ROS, as key signaling molecules, regulate the inflammatory signal in keratinocytes by promoting the production of proinflammatory factors and activating the MAPK and NF- κ B pathways [44]. High levels of ROS have been observed in rosacea and psoriasis [32]. Removing excessive ROS reduces the expression of pro-inflammatory mediators in keratinocytes and alleviates rosacea- and psoriasis-like skin inflammation [44,45]. Here, we found that Nav1.8 was upregulated by TNF α and induced ROS accumulation and production of pro-inflammatory factors in keratinocytes. The addition of mtROS scavenger significantly reduced Nav1.8-C-induced upregulation of pro-inflammatory factors in keratinocytes, indicating that Nav1.8 promoted skin inflammation by driving ROS-mediated inflammatory signaling in keratinocytes. Conduction of ions is the vital channel function of Nav1.8, which subsequently induces action potentials in excitable cells or ATP release in non-excitabile cells [25]. However, several ion channels have been reported to link biological progression through a non-conducting mechanism [46]. In this study, we found that A803467-inhibited Nav1.8 activation did not affect TNF α -induced ROS accumulation and production of pro-inflammatory factors in keratinocytes, suggesting that the Nav1.8 involvement in the inflammatory response in keratinocytes, is independent of its channel function. The C-terminus of ion channels, including the Nav1.8 channel, affects channel function by trafficking the channels to the cell surface [47,48]. Zhou et al. showed that functional Nav1.8 in non-neuronal cell lines is limited, which is attributed to Nav1.8 C-terminus [49]. This partly attributed to the C-terminus-limited Nav1.8 function in keratinocytes.

As a non-channel functional mechanism, some channel proteins have been reported to be involved in biological processes by interacting with functional proteins [46,50]. Using IP-MS, we detected proteins that interacted with Nav1.8 and identified SOD2 as a interaction partner of Nav1.8-C. SOD2 is a key mitochondrial antioxidant that catalyzes superoxide radical dismutation, thereby protecting cells from oxidative damage. Studies have shown that SOD2 expression is downregulated after UVB irradiation, which is linked to ROS-mediated inflammation during skin photoaging [51]. SOD2-ROS signaling is also involved in nitrogen mustard-induced cutaneous inflammation [51]. In this study, we found that Nav1.8 did not affect SOD2 expression but regulated SOD2 activity. SOD2 is an inactive precursor in the cytosol that is imported into the mitochondria where it scavenges ROS [13]. Hsp70 is involved in the mitochondrial import of SOD2 [13], but the precise mechanism remains unclear. Moreover, the deacetylation status is essential for the activation of SOD2. Lysine 68 (K68) is the critical acetylation site regulated by SIRT3 [52,53]. Consistent with these observations, we found that the interaction of Nav1.8-C with SOD2 limited SOD2 activity by preventing SOD2-K68 acetylation and the SOD2 translocation to the mitochondria. However, the precise interaction mechanism needs to be elucidated.

In summary, our study reveals that the upregulation of Nav1.8 expression in keratinocytes is responsible for developing inflammatory skin disorders. The results indicate that Nav1.8 exerts this effect by inducing ROS-mediated proinflammatory signaling by interacting with SOD2 to inhibit SOD2 activation in keratinocytes. Our findings suggest a pivotal role for Nav1.8 in the pathogenesis of inflammatory skin disorders and provide a new theoretical basis for the clinical treatment of these skin disorders, including rosacea and psoriasis.

Author contributions

YZ conducted the investigation, methodology, formal analysis, and visualization and wrote and reviewed and edited the manuscript. LZ, XY,

YW and ZD performed the investigation, methodology and formal analysis. JL and HX provided resources. YL, SX and QD conducted the investigation and clinical phenotyping. YL performed the investigation and reviewed and edited the manuscript. JL provided conceptualization, resources, visualization, supervision, project administration, and funding acquisition and reviewed the manuscript.

Funding

This work was supported by National Natural Sciences Foundation of Hunan province (2020JJ5950). This work was supported by the National Natural Science Foundation of China (81703149, 82173448 and 82073457).

Declaration of competing interest

The authors have declared that no conflict of interest exists.

Data availability

Data will be made available on request.

Appendix A. Supplementary data

Supplementary data to this article can be found online at <https://doi.org/10.1016/j.redox.2022.102427>.

References

- [1] L. Gether, L.K. Overgaard, A. Egeberg, J.P. Thyssen, Incidence and prevalence of rosacea: a systematic review and meta-analysis, *Br. J. Dermatol.* 179 (2018) 282–289, <https://doi.org/10.1111/bjd.16481>.
- [2] F.O. Nestle, D.H. Kaplan, J. Psoriasis Barker, *N. Engl. J. Med.* 361 (2009) 496–509, <https://doi.org/10.1056/NEJMra0804595>.
- [3] A.M. Two, W. Wu, R.L. Gallo, T.R. Hata, Rosacea: part II. Topical and systemic therapies in the treatment of rosacea, *J. Am. Acad. Dermatol.* 72 (2015) 761–770, <https://doi.org/10.1016/j.jaad.2014.08.027>, quiz 771–762.
- [4] B. Feaster, A. Cline, S.R. Feldman, S. Taylor, Clinical effectiveness of novel rosacea therapies, *Curr. Opin. Pharmacol.* 46 (2019) 14–18, <https://doi.org/10.1016/j.coph.2018.12.001>.
- [5] Z. Deng, et al., Keratinocyte-immune cell crosstalk in a STAT1-mediated pathway: novel insights into rosacea pathogenesis, *Front. Immunol.* 12 (2021), 674871, <https://doi.org/10.3389/fimmu.2021.674871>.
- [6] J.M. Leyva-Castillo, et al., Basophil-derived IL-4 promotes cutaneous *Staphylococcus aureus* infection, *JCI Insight* 6 (2021), <https://doi.org/10.1172/jci.insight.149953>.
- [7] D. Jones, Reactive oxygen species and rosacea, *Cutis* 74 (17–20) (2004), 32–14.
- [8] S. Narayanan, A. Hünerbein, M. Getie, A. Jäckel, R.H. Neubert, Scavenging properties of metronidazole on free oxygen radicals in a skin lipid model system, *J. Pharm. Pharmacol.* 59 (2007) 1125–1130, <https://doi.org/10.1211/jpp.59.8.0010>.
- [9] S. Sabnam, H. Rizwan, S. Pal, A. Pal, CEES-induced ROS accumulation regulates mitochondrial complications and inflammatory response in keratinocytes, *Chem. Biol. Interact.* 321 (2020), 109031, <https://doi.org/10.1016/j.cbi.2020.109031>.
- [10] G.S. Shadel, T.L. Horvath, Mitochondrial ROS signaling in organismal homeostasis, *Cell* 163 (2015) 560–569, <https://doi.org/10.1016/j.cell.2015.10.001>.
- [11] K. Yasui, A. Baba, Therapeutic potential of superoxide dismutase (SOD) for resolution of inflammation, *Inflamm. Res. : Off. J. Eur. Histamine Res. Soc. [et al.]* 55 (2006) 359–363, <https://doi.org/10.1007/s00011-006-5195-y>.
- [12] C.T. Nguyen, S.K. Sah, C.C. Zouboulis, T.Y. Kim, Inhibitory effects of superoxide dismutase 3 on Propionibacterium acnes-induced skin inflammation, *Sci. Rep.* 8 (2018) 4024, <https://doi.org/10.1038/s41598-018-22132-z>.
- [13] S. Zemanovic, et al., Dynamic phosphorylation of the C terminus of Hsp70 regulates the mitochondrial import of SOD2 and redox balance, *Cell Rep.* 25 (2018) 2605–2616, <https://doi.org/10.1016/j.celrep.2018.11.015>, e2607.
- [14] G.P. Maiti, et al., SIRT3 overexpression and epigenetic silencing of catalase regulate ROS accumulation in CLL cells activating AXL signaling axis, *Blood Cancer J.* 11 (2021) 93, <https://doi.org/10.1038/s41408-021-00484-6>.
- [15] J. Plenikowska, M. Gabig-Cimińska, P. Mozolewski, Oxidative stress as an important contributor to the pathogenesis of psoriasis, *Int. J. Mol. Sci.* 21 (2020), <https://doi.org/10.3390/ijms21176206>.
- [16] V.S. Tisma, et al., Oxidative stress and ferritin expression in the skin of patients with rosacea, *J. Am. Acad. Dermatol.* 60 (2009) 270–276, <https://doi.org/10.1016/j.jaad.2008.10.014>.
- [17] Q. Zhou, U. Mrowietz, M. Rostami-Yazdi, Oxidative stress in the pathogenesis of psoriasis, *Free Radic. Biol. Med.* 47 (2009) 891–905, <https://doi.org/10.1016/j.freeradbiomed.2009.06.033>.

- [18] H. Keum, et al., Bilirubin nanomedicine alleviates psoriatic skin inflammation by reducing oxidative stress and suppressing pathogenic signaling, *J. Contr. Release : Off. J. Control. Release Soc.* 325 (2020) 359–369, <https://doi.org/10.1016/j.jconrel.2020.07.015>.
- [19] Y. Li, et al., Exploring metformin as a candidate drug for rosacea through network pharmacology and experimental validation, *Pharmacol. Res.* (2021), 105971, <https://doi.org/10.1016/j.phrs.2021.105971>.
- [20] G. Aghahari, et al., Superoxide dismutase 3 inhibits LL-37/CLK-5-mediated skin inflammation through modulation of EGFR and associated inflammatory cascades, *J. Invest. Dermatol.* 140 (2020) 656–665, <https://doi.org/10.1016/j.jid.2019.08.434>, e658.
- [21] C. Han, J. Huang, S.G. Waxman, Sodium channel Nav1.8: emerging links to human disease, *Neurology* 86 (2016) 473–483, <https://doi.org/10.1212/wnl.0000000000002333>.
- [22] D. Jiang, et al., Structural basis for voltage-sensor trapping of the cardiac sodium channel by a death stalker scorpion toxin, *Nat. Commun.* 12 (2021) 128, <https://doi.org/10.1038/s41467-020-20078-3>.
- [23] S. Pabel, et al., Inhibition of Na(V)1.8 prevents atrial arrhythmogenesis in human and mice, *Basic Res. Cardiol.* 115 (2020) 20, <https://doi.org/10.1007/s00395-020-0780-8>.
- [24] M.F. Jarvis, et al., A-803467, a potent and selective Nav1.8 sodium channel blocker, attenuates neuropathic and inflammatory pain in the rat, in: *Proceedings of the National Academy of Sciences of the United States of America*, vol. 104, 2007, pp. 8520–8525, <https://doi.org/10.1073/pnas.0611364104>.
- [25] P. Zhao, et al., Voltage-gated sodium channel expression in rat and human epidermal keratinocytes: evidence for a role in pain, *Pain* 139 (2008) 90–105, <https://doi.org/10.1016/j.pain.2008.03.016>.
- [26] J. Lakoma, R. Rimondini, V. Donadio, R. Liguori, M. Caprini, Pain related channels are differentially expressed in neuronal and non-neuronal cells of glabrous skin of fabry knockout male mice, *PLoS One* 9 (2014), e108641, <https://doi.org/10.1371/journal.pone.0108641>.
- [27] Y. Li, et al., Tranexamic acid ameliorates rosacea symptoms through regulating immune response and angiogenesis, *Int. Immunopharm.* 67 (2019) 326–334, <https://doi.org/10.1016/j.intimp.2018.12.031>.
- [28] L. Riol-Blanco, et al., Nociceptive sensory neurons drive interleukin-23-mediated psoriasiform skin inflammation, *Nature* 510 (2014) 157–161, <https://doi.org/10.1038/nature13199>.
- [29] D. Candas, L. Qin, M. Fan, J.J. Li, Experimental approaches to study mitochondrial localization and function of a nuclear cell cycle kinase, Cdk1, *JoVE : JoVE* 53417 (2016), <https://doi.org/10.3791/53417>.
- [30] T. Buhl, et al., Molecular and morphological characterization of inflammatory infiltrate in rosacea reveals activation of Th1/Th17 pathways, *J. Invest. Dermatol.* 135 (2015) 2198–2208, <https://doi.org/10.1038/jid.2015.141>.
- [31] Y. Su, et al., Interleukin-17 receptor D constitutes an alternative receptor for interleukin-17A important in psoriasis-like skin inflammation, *Science immunology* 4 (2019), <https://doi.org/10.1126/sciimmunol.aau9657>.
- [32] O. Bakar, Z. Demircay, M. Yuksel, G. Haklar, Y. Sanisoglu, The effect of azithromycin on reactive oxygen species in rosacea, *Clin. Exp. Dermatol.* 32 (2007) 197–200, <https://doi.org/10.1111/j.1365-2230.2006.02322.x>.
- [33] S. Mizuguchi, et al., Mitochondrial reactive oxygen species are essential for the development of psoriatic inflammation, *Front. Immunol.* 12 (2021), 714897, <https://doi.org/10.3389/fimmu.2021.714897>.
- [34] B.R. Gardill, R.E. Rivera-Acevedo, C.C. Tung, F. Van Petegem, Crystal structures of Ca(2+)-calmodulin bound to Na(V) C-terminal regions suggest role for EF-hand domain in binding and inactivation, in: *Proceedings of the National Academy of Sciences of the United States of America*, vol. 116, 2019, pp. 10763–10772, <https://doi.org/10.1073/pnas.1818618116>.
- [35] J.E. Greb, et al., Psoriasis, *Nat. Rev. Dis. Prim.* 2 (2016), 16082, <https://doi.org/10.1038/nrdp.2016.82>.
- [36] E. Savio-Galimberti, et al., SCN10A/Nav1.8 modulation of peak and late sodium currents in patients with early onset atrial fibrillation, *Cardiovasc. Res.* 104 (2014) 355–363, <https://doi.org/10.1093/cvr/cvu170>.
- [37] K. Zimmermann, et al., Sensory neuron sodium channel Nav1.8 is essential for pain at low temperatures, *Nature* 447 (2007) 855–858, <https://doi.org/10.1038/nature05880>.
- [38] N.K. Frifelt Wienholtz, et al., Infusion of pituitary adenylate cyclase-activating polypeptide-38 in patients with rosacea induces flushing and facial edema which can be attenuated by sumatriptan, *J. Invest. Dermatol.* (2021), <https://doi.org/10.1016/j.jid.2021.02.002>.
- [39] J. Filtjens, et al., Nociceptive sensory neurons promote CD8 T cell responses to HSV-1 infection, *Nat. Commun.* 12 (2021) 2936, <https://doi.org/10.1038/s41467-021-22841-6>.
- [40] A. Cejudo-Roman, et al., The voltage-gated sodium channel nav1.8 is expressed in human sperm, *PLoS One* 8 (2013), e76084, <https://doi.org/10.1371/journal.pone.0076084>.
- [41] H. Sontheimer, J.A. Black, S.G. Waxman, Voltage-gated Na⁺ channels in glia: properties and possible functions, *Trends Neurosci.* 19 (1996) 325–331, [https://doi.org/10.1016/0166-2236\(96\)10039-4](https://doi.org/10.1016/0166-2236(96)10039-4).
- [42] R.K. Gupta, et al., TWEAK functions with TNF and IL-17 on keratinocytes and is a potential target for psoriasis therapy, *Science immunology* 6 (2021), <https://doi.org/10.1126/sciimmunol.abi8823>.
- [43] A. Srivastava, et al., Cross-talk between IFN- γ and TWEAK through miR-149 amplifies skin inflammation in psoriasis, *J. Allergy Clin. Immunol.* 147 (2021) 2225–2235, <https://doi.org/10.1016/j.jaci.2020.12.657>.
- [44] Y.S. Ryu, et al., Particulate matter induces inflammatory cytokine production via activation of NF κ B by TLR5-NOX4-ROS signaling in human skin keratinocyte and mouse skin, *Redox Biol.* 21 (2019), 101080, <https://doi.org/10.1016/j.redox.2018.101080>.
- [45] G. Aghahari, et al., Superoxide dismutase 3 inhibits LL-37/CLK-5-mediated skin inflammation through modulation of EGFR and associated inflammatory cascades, *J. Invest. Dermatol.* (2019), <https://doi.org/10.1016/j.jid.2019.08.434>.
- [46] F.L. Styles, et al., Kv1.3 voltage-gated potassium channels link cellular respiration to proliferation through a non-conducting mechanism, *Cell Death Dis.* 12 (2021) 372, <https://doi.org/10.1038/s41419-021-03627-6>.
- [47] K. Okuse, et al., Annexin II light chain regulates sensory neuron-specific sodium channel expression, *Nature* 417 (2002) 653–656, <https://doi.org/10.1038/nature00781>.
- [48] J.S. Choi, L. Tyrrell, S.G. Waxman, S.D. Dib-Hajj, Functional role of the C-terminus of voltage-gated sodium channel Na(v)1.8, *FEBS Lett.* 572 (2004) 256–260, <https://doi.org/10.1016/j.febslet.2004.07.047>.
- [49] X. Zhou, et al., A chimeric Nav1.8 channel expression system based on HEK293T cell line, *Front. Pharmacol.* 9 (2018) 337, <https://doi.org/10.3389/fphar.2018.00337>.
- [50] H. Xie, et al., Autophagy induction regulates aquaporin 3-mediated skin fibroblasts aging, *Br. J. Dermatol.* (2021), <https://doi.org/10.1111/bjd.20662>.
- [51] E. Bang, D.H. Kim, H.Y. Chung, Protease-activated receptor 2 induces ROS-mediated inflammation through Akt-mediated NF- κ B and FoxO6 modulation during skin photoaging, *Redox Biol.* 44 (2021), 102022, <https://doi.org/10.1016/j.redox.2021.102022>.
- [52] J. Park, et al., Mitochondrial ROS govern the LPS-induced pro-inflammatory response in microglia cells by regulating MAPK and NF- κ B pathways, *Neurosci. Lett.* 584 (2015) 191–196, <https://doi.org/10.1016/j.neulet.2014.10.016>.
- [53] A.E. Dikalova, et al., Mitochondrial deacetylase Sirt3 reduces vascular dysfunction and hypertension while Sirt3 depletion in essential hypertension is linked to vascular inflammation and oxidative stress, *Circ. Res.* 126 (2020) 439–452, <https://doi.org/10.1161/circresaha.119.315767>.